A

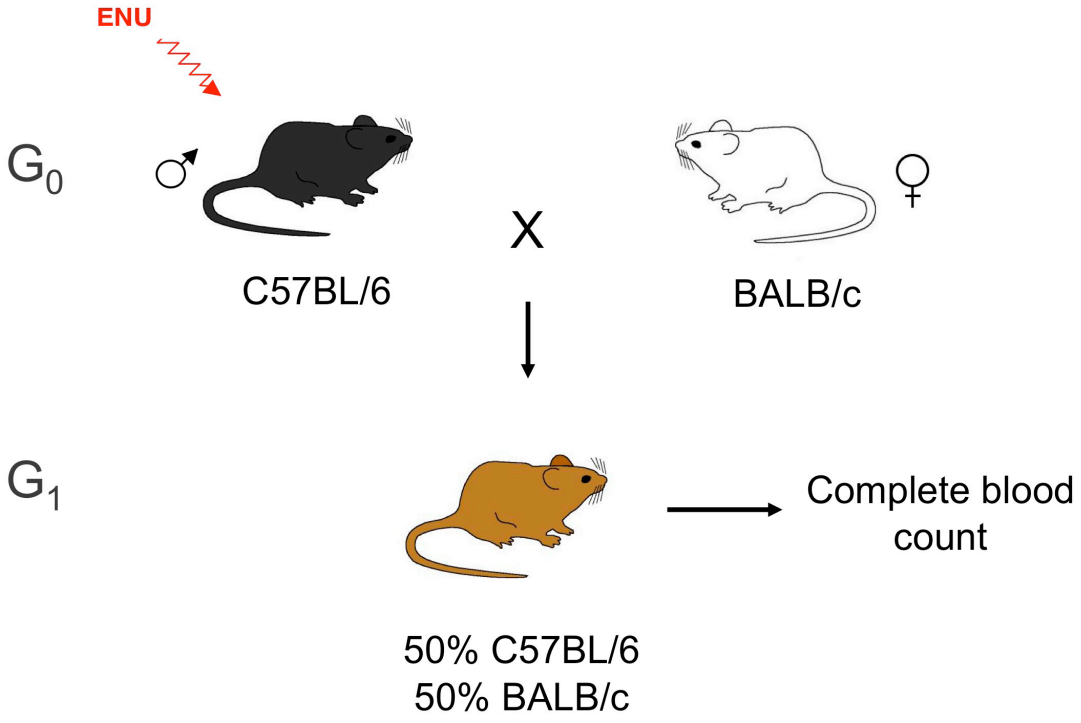

B

Marker	D11Mit4	D11Mit29	rs26924445	rs26908782	D11Mit320	rs26891691	rs6311469	rs28233011	rs26903501	Mice	
Mb	68.42	69.61	70.52	70.76	70.77	70.98	71.16	71.17	72.90	Wild type	Affected
	H	B	B	B	B	B	B	B	B	4	
	B	B	B	H	H	H	H	H	H		8
	H	H	H	B	B	B	B	B	B	1	
	B	B	B	B	B	B	H	H	H	14	
	H	H	H	H	H	H	B	B	B		2
	B	B	B	B	B	B	B	B	H	29	
	H	H	H	H	H	H	H	H	B		47

Figure S1. A N-ethyl-N-nitrosourea (ENU) mutagenesis screen for dominant mutations that cause neutrophilia. (A) Male C57BL/6 mice were injected intra-peritoneally with a total dose of 255 mg/kg of N nitroso-N-ethylurea (ENU, 1g isopac N3385, Sigma-Aldrich) divided into 3 weekly injections. Treated mice were allowed to recover fertility for 8 weeks before mating with untreated BALB/c females to yield first-generation (G1) progeny. At 7 weeks of age, blood from G1 mice was collected from the retroorbital plexus into Microtainer tubes containing EDTA (Becton Dickinson) and the number of neutrophils in the peripheral blood determined using an Advia 2120 automated hematological analyzer (Siemens, Erlangen, Germany). The mutant strain was backcrossed to BALB/c to facilitate mapping and congenic strain production. (B) For mapping, genomic DNA was prepared from tail biopsies and subjected to a genome-wide scan of 550 SNP markers using the Sequenom (San Diego, CA) MassARRAY iPLEX GOLD platform (Australian Genome Research Facility, Parkville, Australia). Mice with greater than 2 x 10^6 neutrophils/mL blood were defined as affected. Products of additional meioses on chromosome 11 were analyzed using SNPs detected with the Amplifluor HT Genotyping System (Millipore, Billerica, MA). For candidate gene sequencing on chromosome 11, genomic DNA was subjected to PCR amplification, treated with ExoSAP-IT (GE Healthcare, Piscataway, NJ) and directly sequenced using BigDye Terminators v3.0 (Life Technologies, Carlsbad, CA). B:BALB/c homozygote; H: heterozygote for BALB/c and C57BL/6J

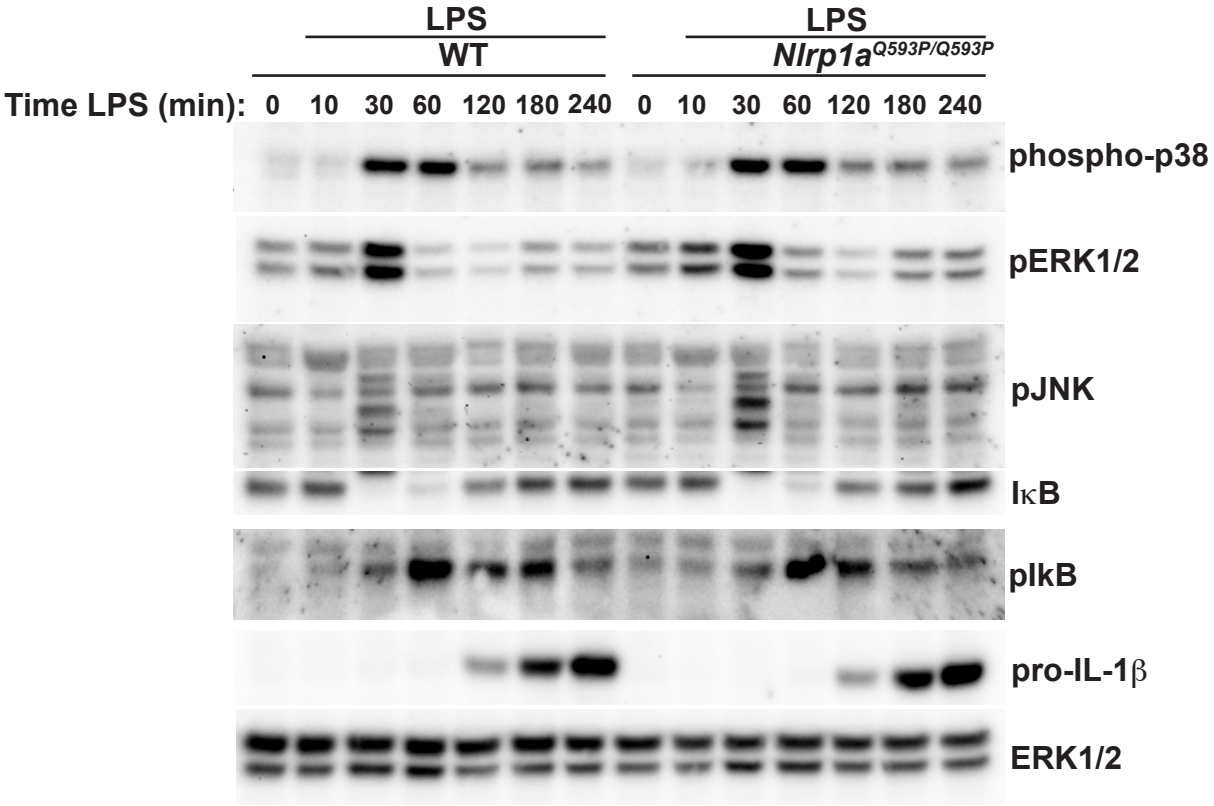

Figure S2. LPS-induced activation of MAP kinases and NFκB is normal in *Nlrp1a*$^{Q593P/Q593P}$ macrophages. Macrophages were stimulated with 1 ng/mL LPS for the indicated times and lysates analysed by immunoblot using antibodies specific to phospho-IκB, IκB, phospho-ERK1/2, ERK1/2, phospho-JNK, phospho-p38 and pro-IL-1β. ERK1/2 is shown as a loading control.

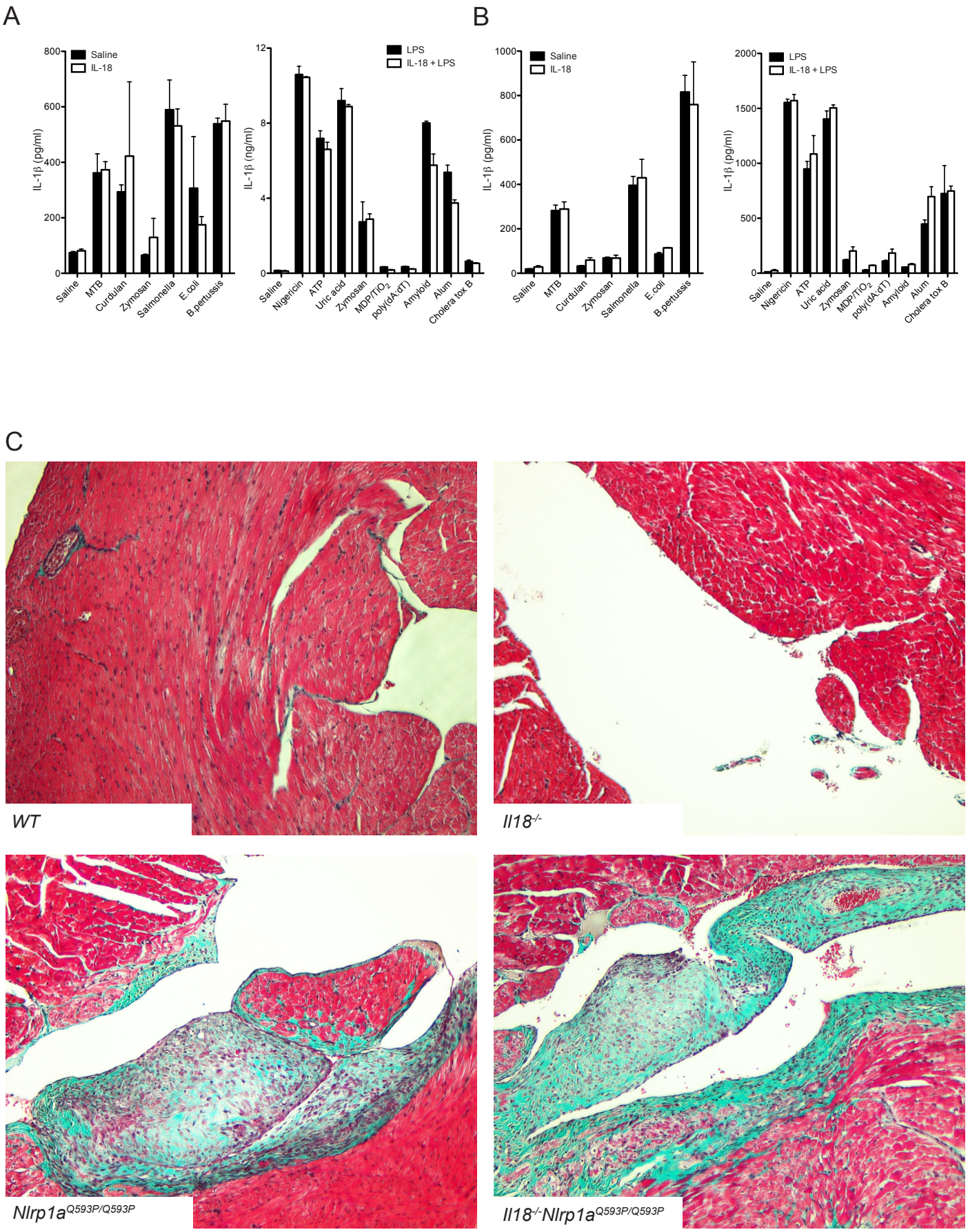

Figure S3. Regulation of inflammation by IL-18. (A&B) IL-18 does not negatively regulate IL-1β production by wild-type myeloid cells. IL-1β production by dendritic cells (A) and macrophages (B) is not modulated by exposure to IL-18. Macrophages or dendritic cells were activated with LPS, then treated with a range of inflammasome activators overnight. IL-1β was measured in supernatant by ELISA. Data represent mean and standard deviation from 3 independent samples. (C) Myocarditis develops in NLRP1a mutant mice in a germ-free environment and in the absence of IL-18. Masson's Trichrome stained cardiac sections were examined under 100x magnification.

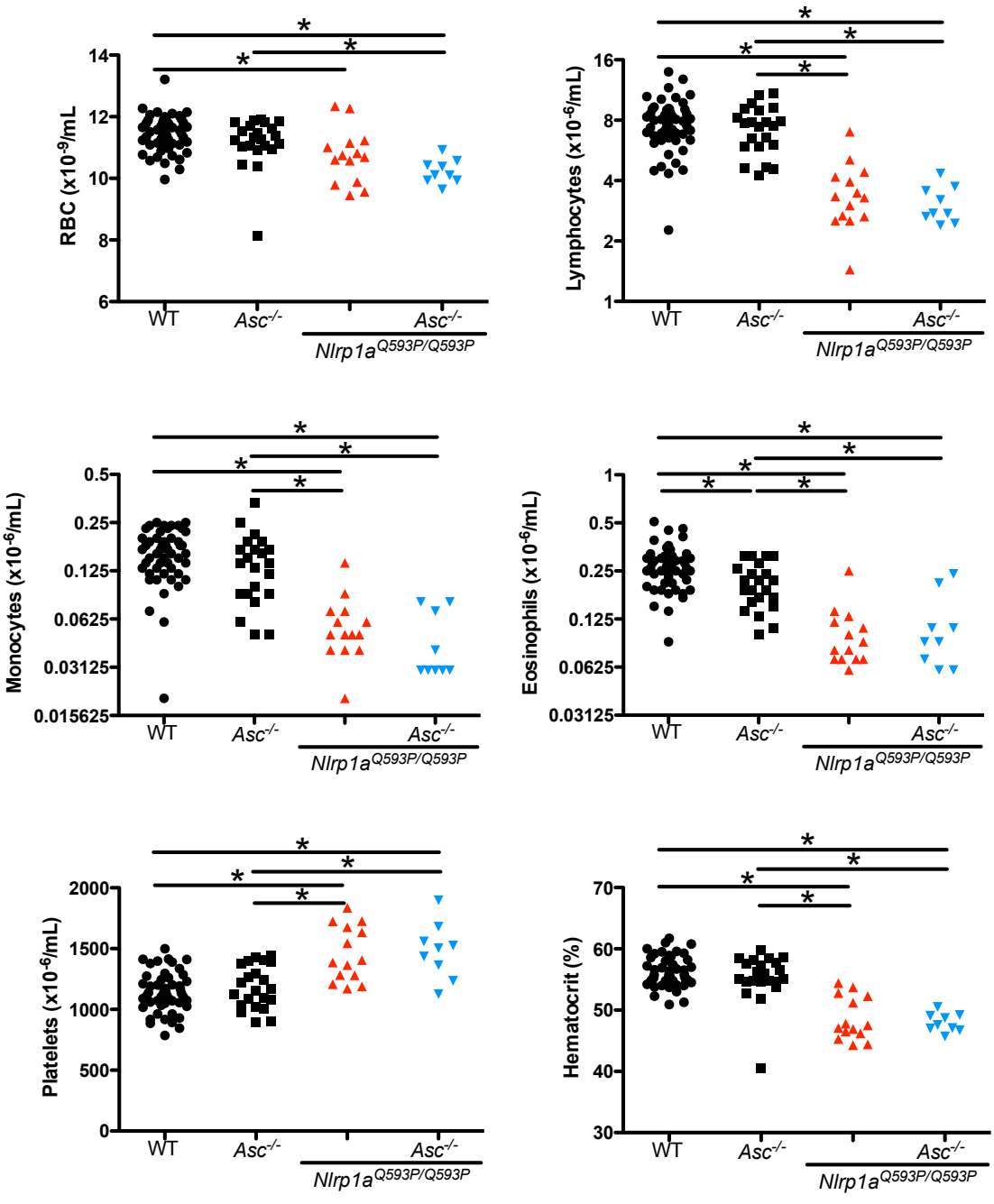

Figure S4. NLRP1 activation induces cytopenia independently of ASC. Peripheral blood was analysed at 7 weeks age.

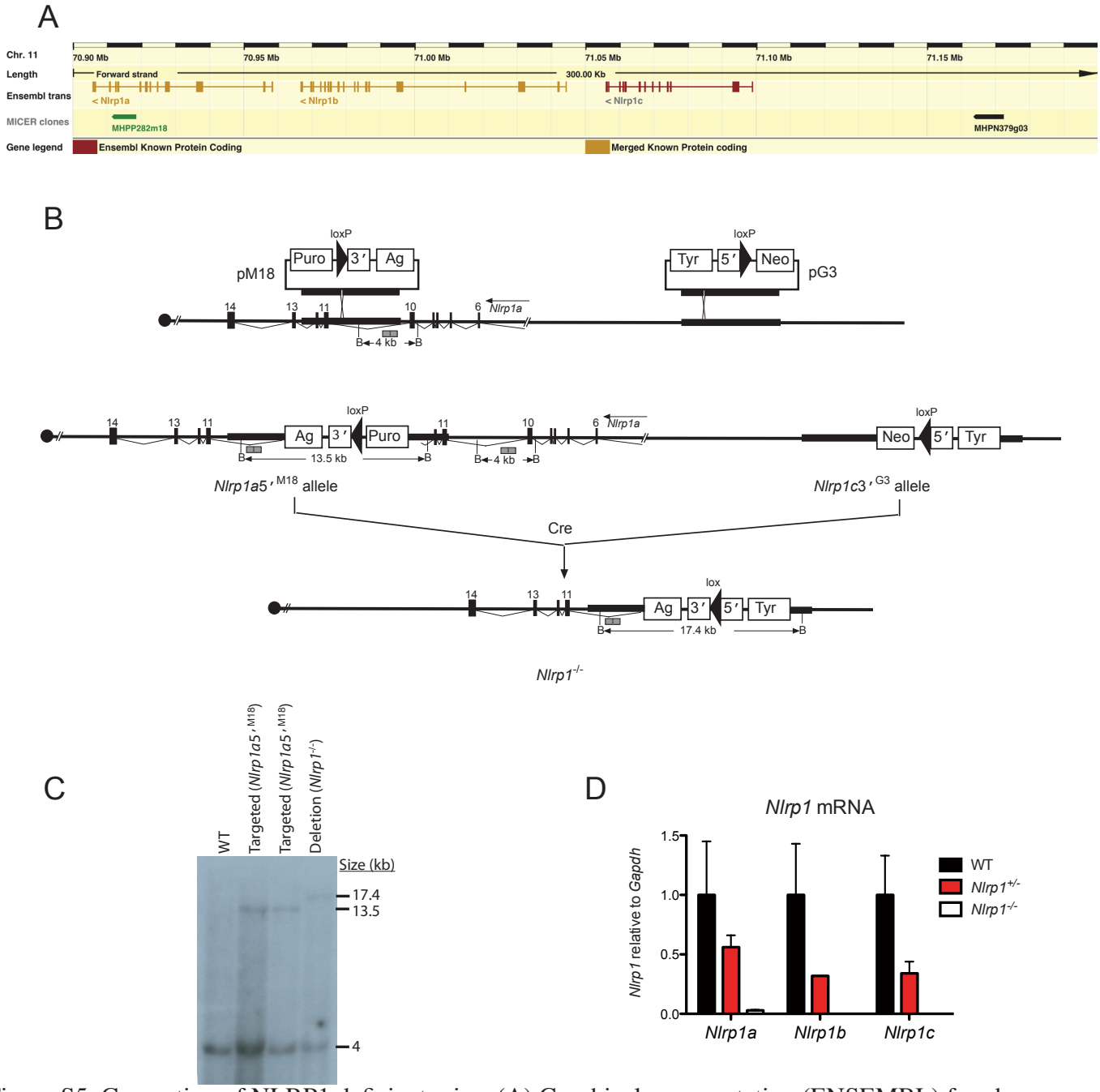

Figure S5. Generation of NLRP1 deficient mice. (A) Graphical representation (ENSEMBL) for chromosome 11 of the mouse genome showing the location of three paralagous *Nlrp1* alleles (*Nlrp1a*, *Nlrp1b* and *Nlrp1c*). Also highlighted are the regions of DNA incorporated into two MICER plasmids which were used for homologous recombination into the mouse genome and subsequent deletion of loxP-flanked DNA (MHPP282m18 referred to as M18, and MHPN379g03 referred to as G3) (Adams et al., *Nature Genetics* 2004). (B) Schematic representation of elements within plasmids M18 and G3, including coat color genes (Ag and Tyr), antibiotic resistance cassettes (Puro and Neo), *loxP* sites and two halves of an HPRT mini-gene that are recombined upon *loxP* site recombination. Each construct was sequentially electroporated into mouse ES cells, followed by a further electroporation of a plasmid expressing Cre recombinase that deletes the entirety of *Nlrp1c*, *Nlrp1b* and the indicated region (Exons 1-10) of *Nlrp1a*. *BamHI* digestion sites are labeled B, with sizes in kb representing fragments detected by a probe highlighted in grey. (C) Using the aforementioned probe, genomic DNA from targeted ES cells was subjected to Southern blot analysis, revealing clones where the M18 insertion and deletion using Cre has occurred as expected. (D) RNA from spleen cells of mice derived from targeted ES cells was subjected to Q-PCR analysis of *Nlrp1* expression using probes from applied biosystems (*Nlrp1a* Mm01241397, *Nlrp1b* Mm01241387, *Nlrp1c* Mm01241401) relative to *Gapdh*.

Adams DJ, Biggs PJ, Cox T, Davies R, van der Weyden L, Jonkers J, Smith J, Plumb B, Taylor R, Nishijima I, Yu Y, Rogers J and Bradley A. *Nature Genetics* 2004;36;8;867-71

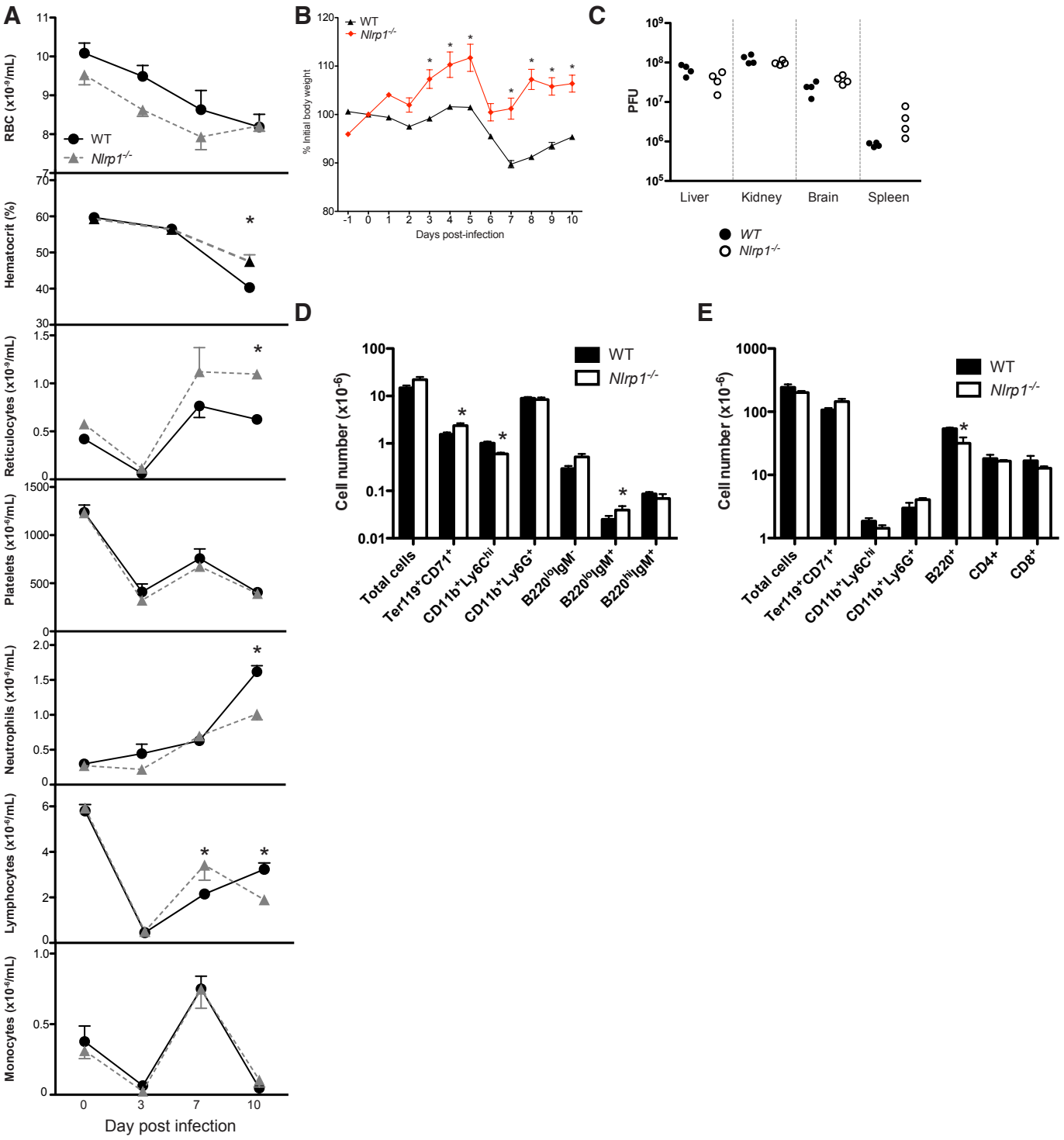

Figure S6. NLRP1 deficiency accelerates recovery from LCMV infection. (A) Enumeration of red blood cells (RBC), reticulocytes, platelets (PLT), neutrophils, lymphocytes and monocytes in the blood of mice infected with LCMV docile. (B) Weight of mice infected with 2 x 10^6 PFU LCMV docile. (C) Viral titers in the liver, kidney, brain and spleen calculated by plaque assay. (D & E) Nucleated cells in the bone marrow (D) and spleen (E) of LCMV-infected mice. *p<0.05, Mean ± sem, n=4.